

**DETC2010-29004**

**EXTERNAL DISTURBANCES AND COUPLING MECHANISMS  
IN UNDERACTUATED HANDS**

**Ravi Balasubramanian\*, Joseph T. Belter, and Aaron M. Dollar**

Department of Mechanical Engineering

Yale University

New Haven, Connecticut 06520.

{ravi.balasubramanian, joseph.belter, aaron.dollar}@yale.edu

**ABSTRACT**

*With the goal of improving the performance of under-actuated robotic hands in grasping, we investigate the influence of the underlying coupling mechanism on the robustness of underactuated hands to external disturbance. This paper identifies unique behaviors in the hand's response as a function of the coupling mechanism and the actuation mode the hand is operated in. Specifically, we show that in conditions when the actuator position is fixed, hands with single-acting mechanisms exhibit a bimodal behavior in contrast to hands with double-acting mechanisms that exhibit a unimodal behavior. We then present an analysis of how these behaviors influence grasping capability of the hand and then discuss implications for underactuated hand design and operation.*

**1 INTRODUCTION**

There has long been a desire to minimize the number of actuators in robotic and prosthetic hands due to constraints on size and mass. This has been accomplished by coupling the motion of joints, with many designs having fewer actuators than degrees of freedom. Such robotic hands, termed “underactuated”, also exhibit passive adaptability between joints and digits; that is, in certain situations, these hands naturally change posture to adapt to the environment. While the performance and design of underactuated hands when driven through internal actuation have been analyzed in prior work [1–5], the behavior of these hands when they

are driven by external forces is still not well understood. This “disturbance response” behavior is the subject of this paper.

Several clever underactuated hand designs have been proposed in prior work. While the hands may differ in the number of fingers and the number of links in each finger, this paper focuses on the differences between the hands in terms of the coupling transmission design and the actuation mode for flexion (curling) and extension (opening) finger motion. There are two primary types of actuating mechanisms: single-acting and double-acting. Single-acting mechanisms control only one of either the flexion or extension of the finger (see Figs. 1a and 1c). This is achieved using an actuator that can only pull (for example, a single cable routing) or push (for example, a plunger), and the reverse motion is achieved using springs. Examples of robotic hands with single-acting mechanisms include the SDM [1], Balance Bar [6], and 100G robotic hands [7].

In contrast, double-acting mechanisms control both the flexion and extension motion of the fingers (see Fig 1d). This is achieved through different methods, such as four-bar linkages, double cable routing, or gears. Note that springs may still be used to ensure mechanism stability and compliance. Examples of robotic hands with double acting mechanisms include the Laval Hands [8,9], SPRING [10], Southampton [11], Graspar [12], BarrettHand [13], and Obrero [14] robotic hands. In addition, some double-acting hands such as the BarrettHand and the Southampton hand feature clutch mechanisms that engage or disengage the

---

\*Contact author

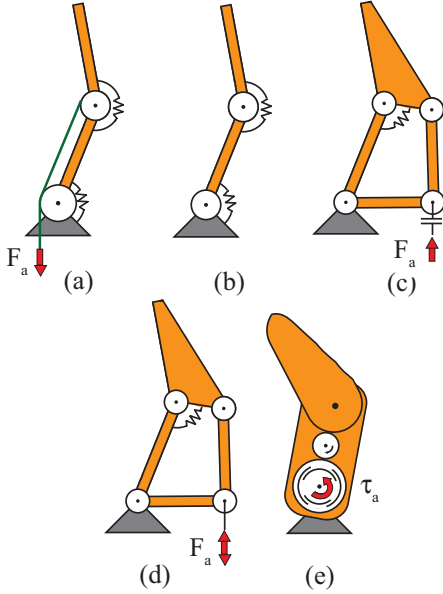


Figure 1. EXAMPLES OF UNDERACTUATED HANDS: (A) SINGLE ACTING CABLE-DRIVEN SYSTEM, (B) SINGLE-ACTING WHEN COUPLING BREAKS DOWN (CABLE SLACK), (C) SINGLE-ACTING WITH EXTRA DEGREE OF FREEDOM (PLUNGER CAN PUSH, BUT NOT PULL), (D) DOUBLE-ACTING LINKAGE-DRIVEN SYSTEM, (E) CLUTCH MECHANISM SYSTEM

joint coupling based on actuation conditions (see Fig. 1e).

The manner in which the underactuated hands reshape in the presence of external forces is important. External forces can arise in several situations, including unplanned collisions, vibration of the base, or changing force from another finger. These events can occur when the hand approaches an object or when the hand is already closed on an object. Forces acting on the phalanxes are transferred through the mechanism all the way back to the actuator. As a result, the effect of these forces is a function of not only the coupling scheme in the mechanism, but also the nature of the actuation, including backdrivability and control mode (for example, force control or position control). While the equilibrium of underactuated grasping in the presence of disturbances has been studied before [15], the influence of the coupling mechanisms on the hand's response is still not clearly understood. A certain disturbance force might result in grasp failure in one coupling and actuation scheme, particularly when are a large number degrees of freedom, and in a more stable grasp in another situation. It is therefore important to analyze how various configurations behave in response to disturbances and use

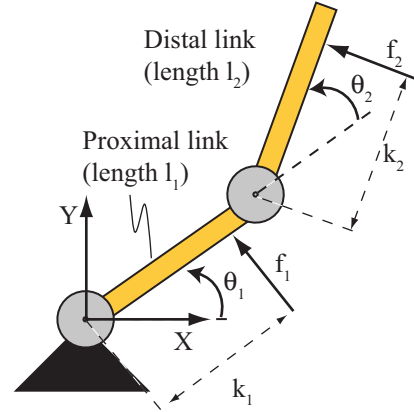


Figure 2. TWO-LINK REVOLUTE-REVOLUTE FINGER. THE ACTUATION CAN BE EITHER A SINGLE-ACTING OR DOUBLE-ACTING MECHANISM (SEE FIG. 1)

this understanding to design the most appropriate coupling and actuation schemes.

In this paper, we first present a framework for studying the response of underactuated hands to external disturbance forces, taking into consideration the kinematics of joint coupling, external forces, and control modes (section 2). Then in section 3, we present results from an analysis of the configuration change of two-link underactuated fingers, incorporating cable-driven systems and linkage driven systems, in response to external forces. We also present how these configuration changes potentially affect a grasp. Finally, in section 4, we present a discussion of the interesting behaviors arising from the combination of control modes and the coupling mechanism and how this analysis can inform the design and operation of underactuated hands.

## 2 FRAMEWORK FOR UNDERACTUATED HAND ANALYSIS

Our framework for analyzing underactuated hands consists of three components: 1) The static equilibrium equations that relate contact forces on the phalanxes with joint torques; 2) The kinematic coupling between the phalanxes and the actuator; 3) The change in robot configuration due to the external forces in the presence of joint coupling. As an example, we consider the flexion and extension behavior of a two-link revolute-revolute finger with a single actuator (see Fig. 2).

### 2.1 Static Equilibrium

The relationship between the contact forces and the net joint torques in the finger (see Fig. 2) may be expressed as

$$\tau = J_c^T f_e, \quad (1)$$

where  $f_e = \begin{pmatrix} f_1 \\ f_2 \end{pmatrix}$  represents the normal contact force on the proximal and distal links,  $\tau = \begin{pmatrix} \tau_1 \\ \tau_2 \end{pmatrix}$  the resulting torque at the joints, and  $J_c \in \mathbb{R}^{2 \times 2}$  the Jacobian that maps between the two spaces. For a two-link mechanism, the Jacobian  $J_c$  can be computed as [2]

$$J_c = \begin{pmatrix} k_1 & 0 \\ k_2 + l_1 \cos \theta_2 & k_2 \end{pmatrix}, \quad (2)$$

where  $k_1$  represents the proximal force location,  $k_2$  the distal force location,  $l_1$  the proximal link length,  $l_2$  the distal link length,  $\theta_2$  the relative angle between the two links. While this formulation assumes that the contact point can slide on the link without friction, friction models can easily be incorporated into this framework. We present a brief discussion of the influence of the contact types on this analysis in section 4.

## 2.2 Kinematics of the Coupling Mechanism

The kinematics of the coupling mechanism may be expressed as a first-order differential equation in the mechanism's configuration  $\theta = \begin{pmatrix} \theta_1 \\ \theta_2 \end{pmatrix}$  and actuator variable  $\theta_a$ . In cable-driven mechanisms, the actuator variable may be defined as the angle traveled by the actuator pulley over which the cable travels, while in linkage driven mechanisms, the actuator variable may be defined as the angle traveled by the actuating link.

For cable driven mechanisms in current underactuated hands such as the SDM hand, the kinematics of the coupling mechanism may be expressed as

$$\Delta \theta_a = r_1 \Delta \theta_1 + r_2 \Delta \theta_2, \quad (3)$$

where  $r_1$  and  $r_2$  represent the pulley radii (assuming unit radius for the actuation pulley).

For four-bar linkage driven mechanisms in current underactuated hands such as the SARAH hand, the kinematics of the coupling mechanism may be expressed as

$$\Delta \theta_a = \Delta \theta_1 + \Delta \theta_2 R, \quad (4)$$

where  $R$  represents the transmission ratio of the mechanism. Note that for a four-bar linkage mechanism, the transmission ratio  $R$  is a function of joint configuration  $\theta$  and link lengths. In this paper, we consider only small joint configuration changes from a given configuration  $\theta$ . Thus,  $R$  is treated as a constant for the instantaneous analysis in this paper.

A closer analysis of (3) and (4) shows that the kinematics of both cable-driven mechanisms and linkage-driven mechanisms can be expressed as

$$J_a \Delta \theta = \Delta \theta_a, \quad (5)$$

where  $J_a = \begin{pmatrix} a_1 & a_2 \end{pmatrix}$  represents the actuator Jacobian of the mechanism. For linkage-driven systems,  $a_1$  equals 1 and  $a_2$  equals  $R$ . For cable-driven systems,  $a_1$  equals  $r_1$  and  $a_2$  equals  $r_2$ . For both types of systems, the transmission ratio may be defined as  $R = a_2/a_1$ . This common structure between the coupling mechanisms of existing underactuation hands induces the hands to behave in a similar fashion when driven by the actuator [2]. However, as will be shown, these mechanisms behave differently in the presence of disturbance forces.

Some double-acting hands like the BarrettHand [13] and the Southampton hand [11] use either clutch or brake mechanisms to enable a multimodal joint coupling. For example, the BarrettHand switches the joint coupling depending on the proximal joint torque value, while the Southampton hand uses brakes to specify the joint coupling. The joint coupling for the BarrettHand may be expressed as:

$$\left. \begin{aligned} \Delta \theta_2 &= \alpha \Delta \theta_1, & \text{if } \tau_1 < \tau_{max} \\ \Delta \theta_1 &= 0, \quad \Delta \theta_2 > 0, & \text{if } \tau_1 > \tau_{max} \end{aligned} \right\}, \quad (6)$$

where  $\tau_{max}$  represents the maximum allowed torque at the proximal joint and  $\alpha$  the fixed non-adaptive coupling ratio between the two joints. Note that the BarrettHand is not backdrivable and is not compliant because of a double-acting worm gear mechanism. Similarly, the Southampton hand uses a rigid coupling mechanism and is non-backdrivable because of the lead-screws that drive the joints. Thus, these hands are rigid to external disturbances. We will not explore such hands with such rigid coupling mechanisms further in this paper.

## 2.3 Robot Configuration Change Due to External Force

An external disturbance force  $f_e$  on the robot can cause a change in configuration  $\Delta \theta$ . The magnitude and direction of  $\Delta \theta$  in the joint configuration space depends on factors such as 1) the joint coupling, 2) the direction, magnitude, and location of the disturbance force, 3) the hand control mode, and 4) joint compliance. This paper explores the change in robot configuration as a function of these factors, specifically exploring how  $\Delta \theta$  varies with force direction (tending to either flex or extend the link), magnitude, and

point of application. We also look at two different control modes for the actuator: force control and position control. To reduce the size of the parameter space, we assume disturbance forces are applied normal to the links (that is, frictionless contacts), and do not vary joint stiffness. We also model external forces as constant, but models where the external force changes with deflection (such as compliant springy contacts) and/or models including geometric constraints imposed by external contacts can also be incorporated using the same framework (albeit with differing resultant behaviors). The contact forces are intentionally kept simple in this paper in order to focus on the hand configuration change.

The configuration change  $\Delta\theta$  for an external force  $f_e$  can be quantified using a Lagrangian view of the work done by the external forces and the energy stored in the springs in the presence of the actuation constraints [16]. Specifically, we can define the Lagrangian  $L$  as

$$L = \Delta W_s + \Delta W_c + \Delta W_a, \quad (7)$$

where  $W_s$  represents the work done on the springs,  $W_c$  the work done by the external forces,  $W_a$  the work done on the actuator.

The work done on the spring  $\Delta W_s = -1/2\Delta\theta^T K_J \Delta\theta$  and work done by the external forces  $\Delta W_c = f_e^T J_c \Delta\theta$  [17] are similar in form for all of the underactuated mechanisms we consider. Here  $K_J = \begin{pmatrix} K_{J1} & 0 \\ 0 & K_{J2} \end{pmatrix}$  represents joint stiffness. The work done on the actuator  $W_a$ , however, takes different forms depending on the control mode the mechanism is driven in (see Table 1). In the force-control mode (that is, actuator force is controlled to be constant while actuator position can vary), the work is “real”, while in the position control mode (that is, actuator position is held fixed and force can vary), the “virtual” work must equal zero [18]. In the work equation for the position control mode,  $p$  is the pretension in the actuating mechanism that ensures mechanism stability prior to the application of the external disturbance  $f_e$ .

By taking derivatives of the Lagrangian with respect to the variables and any Lagrange multipliers, we can derive the static balance equations [16]. Table 1 presents the static balance equations for the two-link mechanism, one for each control mode. Note that these equations predict the instantaneous small changes in hand posture  $\Delta\theta$  from a statically stable configuration as a result of the external force and the actuation mode.

A closer look at the static equations reveals that the system response in the decoupled mode (that is, actuator applies no load or position constraint, such as the case when a tendon goes slack) is shaped primarily by the joint stiffnesses  $K_{J1}$  and  $K_{J2}$ . The system response in the force control mode is shaped by the joint stiffnesses  $K_{J1}$  and  $K_{J2}$ , the constant actuation force  $f_a$ , and pulley radii  $r_1$  and  $r_2$ . Thus, the system response in the force control mode may be viewed as a modified version of the system response in the decoupled mode, since the only difference is work done on the actuator. In contrast, the system response in the position control mode is shaped by the joint stiffnesses  $K_{J1}$  and  $K_{J2}$  and the pulley radii ratio  $R$  (due to the kinematic constraint created by constant cable length), and the actuator pretension  $p$ .

### 3 RESULTS

By using the SDM hand as an exemplar of a hand with a single-acting mechanism and the SARAH hand as an exemplar of a hand with a double-acting mechanism, we now present results from the simulation of the models presented in section 2.3 to compute hand configuration change for external loads. We also include an analysis of the potential impact of such finger deviations on a grasp by analyzing the kinematics of a two-link mechanism. In the interest of keeping the parameter space small, we assumed that there was a force only on the distal joint (that is,  $f_1 = 0$ ), but the core of the framework used for analysis holds for disturbance forces on the proximal link also. Table 2 shows the other parameters used in the analysis.

#### 3.1 Response Variation As a Function of Contact Force Location and Magnitude

The models in section 2.3 permit a quantification of configuration change for different external loads. The results for the double-acting (such as a linkage-driven mechanism) and the single-acting actuation case (such as a cable-driven mechanism) for the decoupled and force-control modes are shown in Figs. 3a and 3b. The results for the double-acting actuation case with position-control mode is shown in Fig. 3c. These contour plots show the change in distal joint configuration  $\Delta\theta_2$  of a two-link mechanism as a function of the magnitude and direction of contact force (horizontal axis) and the force contact location (vertical axis). Note that similar contour plots can be derived for the change in proximal joint configuration  $\Delta\theta_1$ .

As expected, Fig. 3a shows that for the decoupled

Table 1. EFFECT OF CONTROL MODE ON WORK DONE ON ACTUATOR BY EXTERNAL FORCES

| Actuation mode          | Work done on actuator   | Static equations   | Example scenario   |
|-------------------------|---|--|--|
| Force control           | $\Delta W_a = f_a \Delta \theta_a$ <sup>1</sup>                             | $-K\Delta\theta + J_c^T f_e + J_a^T f_a = 0$ (8)   | Maintaining fixed cable tension in SDM hand.   |
| Position control        | Virtual work<br>$\Delta W_a = (\lambda - p)\Delta\theta_a = 0$ <sup>2</sup> | $\left. \begin{aligned} J_a \Delta\theta &= 0 \\ -K\Delta\theta + J_c^T f_e + J_a^T (\lambda - p) &= 0 \end{aligned} \right\} (9)$ | 1) Maintaining fixed cable length in SDM hand; 2) Non-backdrivability in SARAH hand. |
| Decoupled (see Fig. 1b) | $W_a = 0$   | $-K\Delta\theta + J_c^T f_e = 0$ (10)  | Cable slackening in SDM hand.  |

<sup>1</sup>:  $f_a$  is the constant actuation force. <sup>2</sup>:  $\lambda$  is the tendon force resulting from the coupling constraint.

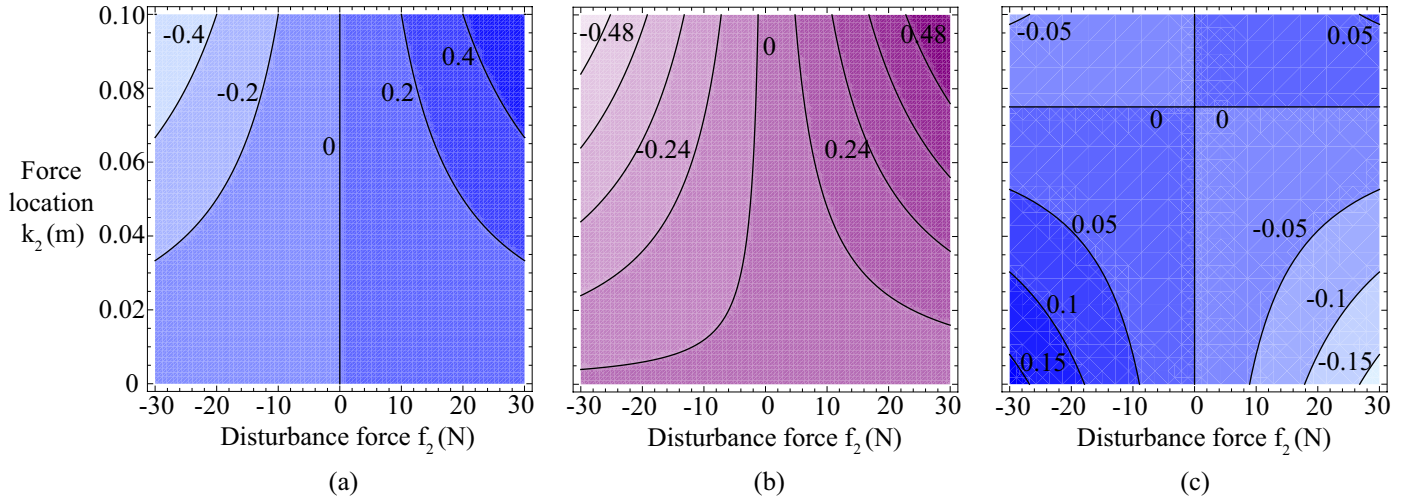


Figure 3. DISTURBANCE RESPONSE OF A TWO-LINK HAND IN (A) DECOUPLED MODE AND (B) FORCE CONTROL MODE. NOTE THAT (A) AND (B) APPLY FOR BOTH SINGLE-ACTING AND DOUBLE-ACTING MECHANISMS. (C) DISTURBANCE RESPONSE OF A TWO-LINK HAND IN POSITION CONTROL MODE WITH A DOUBLE-ACTING MECHANISM. THE CONTOURS SHOW VARIATION IN DISTAL JOINT DEVIATION AS A FUNCTION OF DISTURBANCE FORCE  $f_2$  AND ITS LOCATION  $k_2$ .

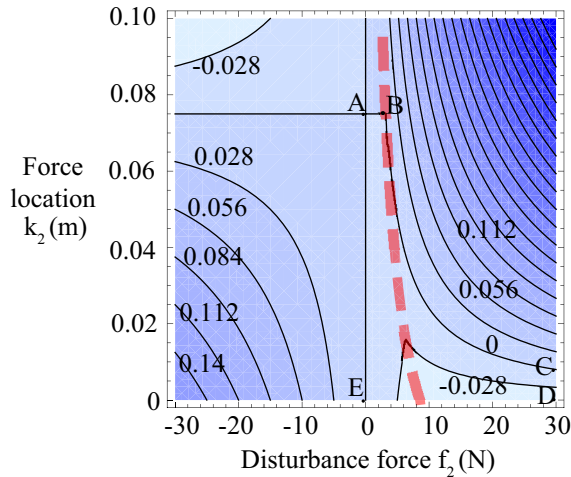
mode, the distal joint closes in ( $\Delta\theta_2$  positive) for flexion external forces and opens out for extending external forces ( $\Delta\theta_2$  negative). The system response in force control mode (see Fig. 3b) is similar to the system response in the decoupled mode, except that the work done on the actuator slightly “warps” the contours. For the double-acting mechanism in position control mode (see Fig. 3c), we see a critical distal force location  $k_2$  at which the mechanism does not move ( $\Delta\theta_2 = 0$ ) for any external force, indicating that the mechanism is extremely stiff at that force location. This location has been termed the equilibrium point for the

mechanism in prior work [2, 19].

The results for the single-acting actuation case (such as a cable-driven mechanism) in position control mode are shown in Fig. 4. This plot shows the change in distal-joint configuration change  $\Delta\theta_2$  of a single-acting two-link mechanism in position control mode with the joint coupling given by (5). The overall response of the system is shaped by the joint stiffnesses  $K_{J1}$  and  $K_{J2}$ , the pulley radii ratio  $R$  (due to the kinematic constraint created by constant cable length), and actuator pretension. The system response is essentially a hybrid between the decou-

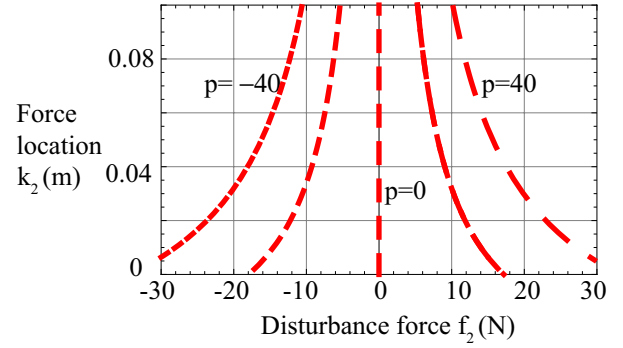
Table 2. SYSTEM PARAMETERS

|   |              |
|---|--------------|
| Proximal joint stiffness $K_{J1}$               | 1 Nm/rad     |
| Distal joint stiffness $K_{J2}$                 | 5 Nm/rad     |
| Proximal and distal link length $l_1$ and $l_2$ | 0.1 m        |
| Proximal pulley radius $r_1$                    | 0.02 m       |
| Pulley radii ratio $R$                          | 0.6 m        |
| Proximal joint configuration $\theta_1$         | $\pi/10$ rad |
| Distal joint configuration $\theta_2$           | $\pi/3$ rad  |
| Cable pretension $p$                            | 10 N         |
| Cable actuation force $f_a$                     | 10 N         |
| External force on proximal link $f_1$           | 0 N          |


 Figure 4. DISTURBANCE RESPONSE OF AN SINGLE-ACTING TWO-LINK HAND IN POSITION CONTROL MODE: VARIATION IN DISTAL JOINT DEVIATION AS A FUNCTION OF DISTURBANCE FORCE  $f_2$  AND ITS LOCATION  $k_2$ .

pled mode (right of the dashed red line) and double-acting mechanism in position control mode (left of the dashed line) seen in Figs. 3a and 3c. The dashed (red) line represents the combination of force magnitude  $f_2$  and location  $k_2$  at which the inter-joint coupling breaks down (for example, the cable going slack in the SDM hand). This dashed line is a function of the tendon tension ( $p=10$  N in this example), and would lie on the  $f_2 = 0$  line if the pretension  $p$  was zero.

To the left of the dashed line, we have a  $\Delta\theta_2 = 0$  contour line when  $f_2 = 0$ , and there is an equilibrium point when  $\Delta\theta_2 = 0$  for any external force, just as in the case


 Figure 5. CONTACT FORCE AND LOCATION COMBINATIONS THAT NULLIFY THE PRETENSION  $p$  IN THE ACTUATOR.

of position control for a double-acting system (see Fig. 3c). But there exists a  $\Delta\theta_2 = 0$  contour to the right of the dashed line also, due to the flexion motion of the distal link for flexion forces in the absence of joint coupling. The transition from a (coupled) position control mode to a decoupled mode produces interesting behavior when either  $k_2$  or  $f_2$  is small (region ABCDE in Fig. 4). The distal joint changes from flexion to extension to flexion in a small force range with force location  $0.04 \text{ m} < k_2 < 0.075 \text{ m}$ . Note that a similar contour plot can be drawn for proximal link deviation  $\Delta\theta_1$  also.

Fig. 5 shows the combination of external force on the distal link and its location that nullifies a pre-existing actuation force (varied here between  $p = -40$  N and  $p = 40$  N). Note that pretension can be positive or negative for double-acting systems, but can be either only positive or only negative for single-acting systems. The contours in this plot are similar to the dashed red line in Fig. 4.

### 3.2 Variation of the Equilibrium Point in Position Control Mode

As noted in Fig. 3c, there is a critical value of force location  $k_2$ , called the equilibrium point, at which the under-actuated hand does not move ( $\Delta\theta = 0$ ) in position control mode. The equilibrium point  $e$  is a function of the mechanism design parameters such as proximal link length  $l_1$ , the pulley radii ratio  $R$ , and distal joint angle  $\theta$ , and has the form  $e = l_1 R \cos\theta_2 / (1 - R)$ . Fig. 6 shows that the equilibrium point moves distal rapidly as the pulley radii ratio  $R$  increases toward unity (for fixed distal joint angle  $\theta_2 = \pi/3$ ). This indicates that the equilibrium point could be beyond the distal link length. In contrast, the equilibrium point moves proximal on the distal link as the pulley radii ra-

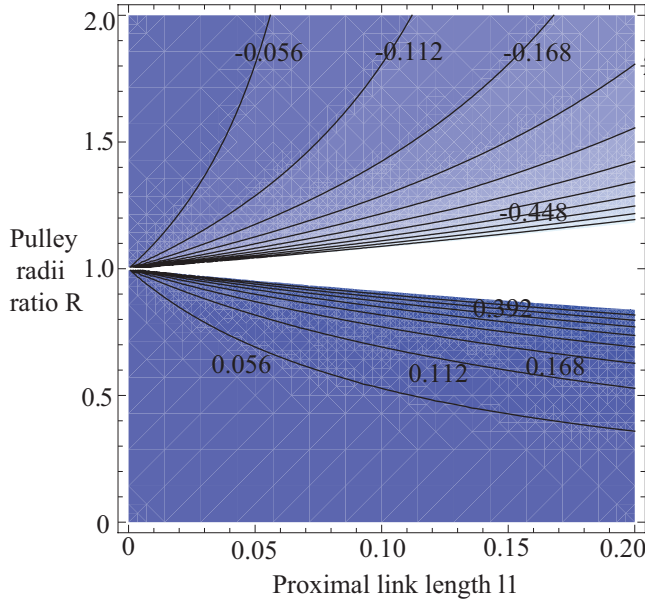


Figure 6. VARIATION OF THE EQUILIBRIUM POINT (CONTOURS) AS A FUNCTION PROXIMAL LINK LENGTH  $l_1$  AND THE PULLEY RADII RATIO  $R$ .

ratio  $R$  decreases toward unity, indicating that the equilibrium point is below the distal joint.

### 3.3 Grasping Behaviors Arising from Hand Configuration Change

Fig. 7 shows the joint configuration change space (for the two-link finger) split into four regions depending on the direction of potential fingertip movement in the X-direction and proximal and distal joint configuration change. The regions represent four behaviors: 1) Squeezing, 2) Caging, 3) Ejection, and 4) Release. Table 3 presents the potential effect of these behaviors on a grasp. Note that prior work in grasping has also explored ejection [2, 20] (albeit in a different form), caging [21], and hold [22] behaviors.

However, a configuration change of an arbitrary direction is not possible in underactuated hands. When underactuated hands are operated in force control mode, then the direction of proximal or distal joint motion depends primarily on the direction of external force. The direction of motion of the proximal joint and distal joint would be identical, indicating a positive slope in the joint configuration space. The exact magnitude of the slope would depend on the relative magnitudes of joint compliance. Thus, the hand would exhibit release behavior for extending forces on the distal link that overcome the cable tension and squeeze behavior for flexion forces on the distal link (see Fig. 8a).

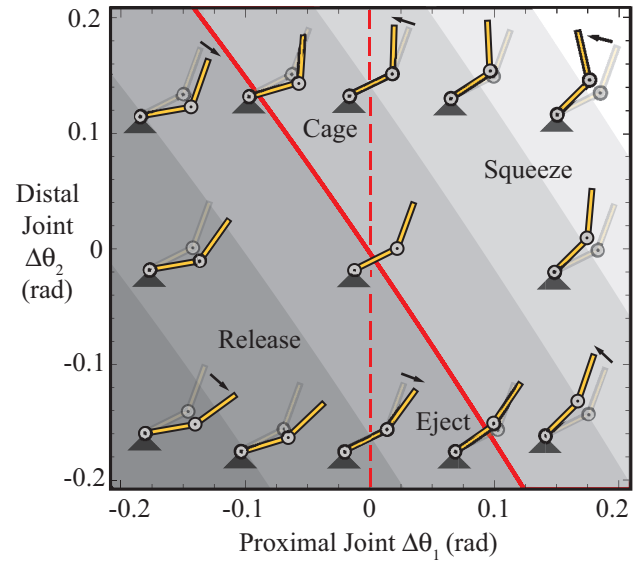


Figure 7. GRASPING BEHAVIORS OF A TWO-LINK FINGER AS A FUNCTION OF JOINT DEFLECTION. THE FINGERTIP HAS DISPLACEMENT ALONG THE NEGATIVE X DIRECTION IN THE REGION TO THE RIGHT OF THE RED SOLID LINE.

Table 3. ROBOT HAND BEHAVIORS AND EFFECT ON A GRASP

| Behavior | Fingertip and joint motions                                 | Potential effect on grasp  |
|----------|---|--|
| Squeeze  | Negative X-motion; both joints curl in                      | Enveloping object with potentially multiple contacts.  |
| Caging   | Negative X-motion; distal joint curls, proximal joint opens | Enveloping object with potential distal contact. Proximal contact weakens. Tends to pull object inward.                          |
| Ejection | Positive X-motion; proximal joint curls, distal joint opens | Potential contact with proximal phalanx, but distal joint moves away potentially breaking contact. Tends to push object outward. |
| Release  | Positive X-motion; both joints open                         | Both phalanges potentially break contact.  |

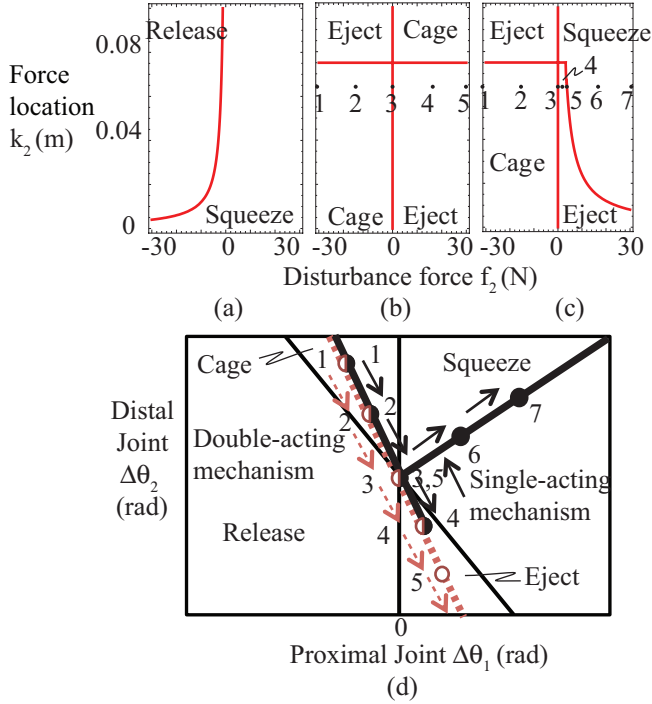


Figure 8. RESPONSE BEHAVIOR OF TWO-LINK FINGER IN A) FORCE CONTROL MODE, B) DOUBLE-ACTING POSITION CONTROL MODE, AND C) SINGLE ACTING POSITION CONTROL MODE TO EXTERNAL DISTURBANCE, D) GRASPING BEHAVIOR OF THE SINGLE-ACTING AND DOUBLE-ACTING MECHANISMS WHEN VIEWED IN JOINT CONFIGURATION-CHANGE SPACE. THE NUMBERED LOCATIONS CORRESPOND TO A VARIATION IN EXTERNAL LOAD FROM THE EXTENSION DIRECTION TO THE FLEXION DIRECTION INDICATED IN (B) AND (C).

However, we get interesting behaviors when the hand is operated in position control mode. Figs. 8b and 8c show the qualitative behavior of single-acting and double-acting underactuated hands to external disturbances when operated in position control mode with the parameters in Table 2. We notice that double-acting mechanisms exhibit caging and ejection behaviors only, depending on the distal force location and magnitude. In contrast, we notice that the single-acting mechanism exhibits caging, ejection, and squeezing behaviors, depending on the external force location and magnitude. Note that these grasping behaviors arising from configuration changes are a function of joint configuration, the coupling mechanism, the number of degrees of freedom in the finger, and external constraints, and the system will respond differently as the parameters change.

## 4 DISCUSSION

One of the goals of our research is to build underactuated robotic hands that offer near-perfect grasping capability in different scenarios. Most previous studies of underactuated hands have explored design issues focused on favorable behavior when the hands are actuated internally (force control mode; see Table 1) [1–5].

Even though we consider only a simple two-link finger in the absence of external constraints in this paper, a close analysis of these systems in position control mode reveals interesting aspects of their behavior. Note that operating a robotic hand in position control mode is analogous to using non-backdriveable transmissions, which is advantageous from a power consumption standpoint. We believe that outlining the behaviors seen in these examples will offer a better understanding the behavior of underactuated hands with more degrees of freedom and in the presence of external constraints.

### 4.1 Bimodal Response of Single-Acting Underactuated Hands In Position Control Mode

While double-acting mechanisms offer a smooth variation in response in position control mode (see Fig. 3c), single-acting mechanisms offer a bimodal response in position control mode (see Fig. 4). Specifically, single-acting hands like the SDM hand in position control mode behave similar to double-acting mechanisms when the cable is taut. However, a sufficiently large external force in the flexion direction can cause the cable to go slack, and thus eliminate the coupling between the two joints. In this decoupled mode, the hand behaves like a passive compliant two-link mechanism and naturally complies with the external force. The external load at which the transition from the position control mode to the decoupled mode occurs is determined by the pretension in the actuation mechanism (see Figs. 4 and 5).

### 4.2 Grasping Behaviors In Underactuated Hands

The grasping behaviors of underactuated hands have been analyzed in several contexts, such as the robustness to uncertainty in hand position relative to the object [23], the sliding of the hand on the object [2, 24], inadvertent contact forces [25], and adaptability [3–5]. In section 3.3, we presented a novel approach to qualifying small hand movements in response to external disturbances in the context of grasping. Specifically, we use the inward movement of the fingertip and distal joint flexion to distinguish hand be-

haviors such as squeezing and caging which tend to wrap the fingers around an object. In contrast, behaviors such as ejection and release tend to unwrap the fingers from the object. Note that this approach of using fingertip motion to qualify a grasping motion depends on the instantaneous joint configuration and the link lengths.

Using this metric over the space of hand configuration changes, we noticed that current underactuated hands in position control mode switch between different behaviors (good and bad) depending on circumstances. Specifically, hands with double-acting mechanisms produce only caging and ejection behavior. Furthermore, they exhibit ejection behavior even for flexion disturbance forces (see Fig. 8b and 8d). Alternatively, hands with single-acting mechanisms like the SDM hand produce caging, ejection, and squeeze behavior (see Fig. 8c and 8d). The squeeze behavior occurs when the joint coupling breaks down and is good for grasping since the hand complies with the external load in a favorable direction. Interestingly, hands with single-acting mechanisms produce an ejection behavior for small external loads (region ABCDE in Fig. 4), but transition into squeeze behavior for larger forces. If the ejection behavior for small loads (region ABCDE) is to be eliminated in cable-driven systems, we infer from Figs. 4 and 5 that the pretension must be zero. In such a condition, any flexion load will cause the mechanism to enter the squeeze behavior. Note that a zero pretension in the actuation mechanism is not always possible, particularly when the hand is already applying forces to a grasped object. More work is required to determine how to get advantageous behavior from underactuated hands in position control mode for arbitrary external loads, particularly in the presence of external constraints and as the number of degrees of freedom increases.

#### 4.3 Effect of Equilibrium Point on Grasping Behaviors

The equilibrium point has been used in previous work as the point towards which a precision grasp's contacts can slide (when internally actuated) for the grasp to become stable [2]. Thus, underactuated hands have been designed to locate the equilibrium point within the distal link, without which the object may be ejected. From our analysis of the response of the fingers to external disturbance (see Figs. 8b and 8c), we notice that another aspect of the equilibrium point may be exploited as well. Both the double-

acting and single-acting mechanisms in position control mode (see Figs. 8b and 8c) transition between different behaviors (caging and ejection in this instance) at the equilibrium point. Thus, the finger could be designed to place the equilibrium point so as to maximize the areas of cage and squeeze behaviors across the mechanism's joint configuration space. More work is required to provide a unified view of underactuated grasping in the light on internal actuation and external disturbances.

It is also interesting that since joint stiffnesses do not affect the equilibrium point, they can be chosen based on other factors. For instance, the ratio of the joint stiffnesses can be set in order to ensure that the proximal joint closes in on an object at a faster rate than the outer joint when actuated to ensure maximum grasping ability in the presence of uncertainty (as is suggested in [26]).

#### 4.4 Modeling of Contact Forces

The external forces that we have used in this paper have been intentionally kept simple so that the analysis can focus on the deflections of the mechanism. Specifically, we have used contact forces that slide on the links [2] and remain constant as the mechanism changes configuration. However, note that the choice of contact force model does not affect the core of the framework used for analysis. External forces that arise from compliant and sticky contacts can easily be included in the Lagrangian formulation [16].

While our paper has quantified the configuration changes of the hand as a function of external loads, we have only shown qualitatively how such deflections may influence grasps. Once the kinematic constraints arising from contacts with objects and the environment are included, our framework for analyzing hand configuration change will inform how the contact forces change and influence object stability. This will then permit us to leverage prior work in quantifying grasp stability [2, 27].

#### ACKNOWLEDGMENT

The authors thank Lael Odhner for interesting discussions on Lagrangian formulation of mechanical systems.

#### REFERENCES

- [1] Dollar, A. M., and Howe, R. D., 2006. "A robust compliant grasper via shape deposition manufacturing". *ASME/IEEE Trans. on Mechatron.*, **11**(2), pp. 154–161.
- [2] Birglen, L., Laliberté, T., and Gosselin, C., 2008. *Underactuated Robotic Hands*. Springer.

- [3] Hirose, S., and Umetani, Y., 1978. “The development of soft gripper for the versatile robot hand”. *Mechanism and Machine Theory*, **13**, pp. 351–359.
- [4] Rakic, M., 1989. “Multifingered hand with self-adaptability”. *Robotics and Computer-Integrated Manufact.*, **3**(2), pp. 269–276.
- [5] Rovetta, A., 1981. “On functionality of a new mechanical hand”. *ASME J. Mechanical Design*, **103**, pp. 277–280.
- [6] Kamikawa, Y., and Maeno, T., 2008. “Underactuated five-finger prosthetic hand inspired by grasping force distribution of humans”. In Proc. IEEE/RSJ Internat. Conf. on Intell. Robots and Sys., pp. 717–722.
- [7] Kaneko, M., Higashimori, M., Takenaka, R., Namiki, A., and Ishikawa, M., 2003. “The 100G capturing robot too fast to see”. *ASME/IEEE Trans. on Mechatronics*, **8**(1), pp. 37–44.
- [8] Gosselin, C., and Laliberté, T., 1996. Underactuated mechanical finger with return actuation. US Patent 5 762 390.
- [9] Laliberté, T., and Gosselin, C., 2002. Actuation system for highly underactuated gripping mechanism. US Patent 6 505 870.
- [10] Carrozza, M. C., Suppo, C., Sebastiani, F., MASSA, B., Vecchi, F., Lazzarini, R., Cutkosky, M. R., and Dario, P., 2004. “The spring hand: Development of a self-adaptive prosthesis for restoring natural grasping”. *Autonomous Robots*, pp. 125–141.
- [11] Crowder, R. M., Dubey, V. N., Chappell, P. H., and Whatley, D. R., 1999. “A multi-fingered end effector for unstructured environments”. In Proc. IEEE Internat. Conf. on Robotics and Automation, pp. 3038–3043.
- [12] Crisman, J. D., Kanojia, C., and Zeid, I., 1996. “Graspar: A flexible, easily controllable robotic hand”. *IEEE Robotics and Automation Magazine*, pp. 32–38.
- [13] Townsend, W. T., 2000. “The barretthand grasper—programmably flexible part handling and assembly”. *Industrial Robot: An International Journal*, **27**(3), pp. 181–188.
- [14] Torres-Jara, E., 2005. “Obrero: A platform for sensitive manipulation”. In Proc. IEEE-RAS Internat. Conf. on Humanoid Robots, pp. 327–332.
- [15] Kragten, G. A., Kool, A. C., and Herder, J. L., 2009. “Ability to hold grasped objects by underactuated hands: performance prediction and experiments”. In Proc. of IEEE Internat. Conf. Robotics and Automat., pp. 2493–2498.
- [16] Inoue, T., and Hirai, S., 2008. *Mechanics and Control of Soft-fingered Manipulation*. Springer.
- [17] Craig, J. J., 1989. *Introduction to Robotics*. Addison Wesley.
- [18] Murray, R. M., Li, Z. X., and Sastry, S. S., 1994. *A Mathematical Introduction to Robotic Manipulation*. CRC Press.
- [19] Rizk, R., Krut, S., and Dombre, E., 2007. “Grasp-stability analysis of a two-phalanx isotropic underactuated finger”. In Proc. IEEE/RSJ Internat. Conf. on Intell. Robots and Sys., pp. 3289–3294.
- [20] Begoc, V., Durand, C., Kurt, A., Dombre, E., and Pierrot, F., 2006. “On the form-closure capability of robotic underactuated hands”. In Proc. of the Internat. Conf. on Control, Automation, Robotics, and Vision, pp. 2011–2018.
- [21] Diankov, R., Srinivasa, S., Ferguson, D., and Kuffner, J., 2008. “Manipulation planning with caging grasps”. In Proc. of IEEE Internat. Conf. on Humanoid Robots, pp. 285–292.
- [22] Kragten, G. A., and Herder, J. L., 2010. “The ability of underactuated hands to grasp and hold objects”. *Mechanism and Machine Theory*, **45**, pp. 408–425.
- [23] Dollar, A. M., and Howe, R. D., 2006. “Joint coupling design of underactuated grippers”. In Internat. Design Engineering Technical Conf and Computers and Information in Engineering Conf., pp. 903–911.
- [24] Kaneko, M., and Hayashi, T., 1993. “Standing-up characteristic of contact force during selfposture changing motions”. In Proc. of the IEEE Internat. Conf. on Robotics and Automation, pp. 202–208.
- [25] Dollar, A. M., Jentoft, L., Gao, J. H., and Howe, R. D., 2010. “Contact sensing and grasping performance of compliant hands”. *Autonomous Robots*, **28**(1), pp. 65–75.
- [26] Dollar, A. M., and Howe, R. D., 2005. “Towards grasping in unstructured environments: Grasper compliance and configuration optimization”. *Adv. Robotics*, **19**(5), pp. 523–544.
- [27] Mason, M. T., 2001. *Mechanics of Robotic Manipulation*. MIT Press.